

Crystal structure of Lyme disease antigen outer surface protein A complexed with an Fab

HONG LI*†, JOHN J. DUNN*, BENJAMIN J. LUFT‡, AND CATHERINE L. LAWSON*§

*Biology Department, Brookhaven National Laboratory, Building 463, Upton, NY 11973; and ‡Division of Infectious Diseases, School of Medicine, State University of New York, Stony Brook, NY 11794

Communicated by Paul B. Sigler, Yale University, New Haven, CT, February 12, 1997 (received for review, November 20, 1996)

ABSTRACT OspA (outer surface protein A) is an abundant immunogenic lipoprotein of the Lyme disease spirochete *Borrelia burgdorferi*. The crystal structure of a soluble recombinant form of OspA was solved in a complex with the Fab fragment of mouse monoclonal antibody 184.1 and refined to a resolution of 1.9 Å. OspA has a repetitive antiparallel β topology with an unusual nonglobular region of “freestanding” sheet connecting globular N- and C-terminal domains. Arrays of residues with alternating charges are a predominant feature of the folding pattern in the nonglobular region. The 184.1 epitope overlaps with a well conserved surface in the N-terminal domain, and a hydrophobic cavity buried in a positively charged cleft in the C-terminal domain is a potential binding site for an unknown ligand. An exposed variable region on the C-terminal domain of OspA is predicted to be an important factor in the worldwide effectiveness of OspA-based vaccines.

Lyme disease is a progressive infection resulting from inoculation of the spirochete *Borrelia burgdorferi* into the skin by a feeding tick, usually *Ixodes* species (1). Dissemination occurs early and can produce a wide array of clinical manifestations. Because some individuals are initially asymptomatic, there is no objective sign or laboratory abnormality that can universally identify infection. Left untreated, infection can eventually lead to serious joint, neurologic, cardiac, and skin abnormalities.

Two basic lipoproteins with 53% sequence identity are abundant proteins of cultured *B. burgdorferi* spirochetes (2). OspA (outer surface protein A, 31 kDa) and OspB (34 kDa) are encoded by tandem genes located on a 49-kb linear plasmid and are transcribed in a single transcriptional unit (3, 4); their natural biological functions are unknown. Although several studies suggest that the predominant location of these antigens is periplasmic, they are also found on the fluid outer membrane (5–8). OspA has been shown to be present when the spirochete is dormant in the tick midgut but is no longer detected after rapid division and dissemination to the tick salivary glands during a blood meal (9). This may explain why the natural immune response to OspA develops only in a minority of Lyme disease patients, and usually only late in the course of the disease. Preliminary studies have shown that vaccines based on OspA can induce protective immunity in mammals (10–12). Blockage of spirochete transmission from the tick vector to the mammalian host by anti-OspA antibodies appears to be the main mechanism of protection (13). Phase III trials to assess the effectiveness of recombinant OspA vaccines in humans are in progress (14, 15).

A fully successful vaccine will require delineation of neutralizing epitopes of OspA and their variation across the range of Lyme-disease-causing *Borrelia* (16, 17). We initiated structure determination of OspA (from strain B31) to aid in vaccine design and to begin to elucidate protein function. Although OspA normally has a lipidated N-terminal cysteine to provide a membrane anchor (18), a recombinant unlipidated form is soluble in aqueous solution and is still recognized by antibodies from Lyme disease patients (19). Efforts to crystallize recombinant OspA by itself failed, but crystals of the protein complexed with the antigen-binding fragment of a murine monoclonal antibody (Fab 184.1) were readily obtained (20). The structure was solved by a combination of molecular replacement and multiple isomorphous replacement methods using diffraction data collected with synchrotron radiation (see Table 1 for details). We report herein a refined atomic model for the complex at a resolution of 1.9 Å (see Fig. 1 for refinement details). OspA has a number of intriguing features, including a novel folding pattern that incorporates alternating charge arrays into antiparallel β -sheet, a potential ligand binding site, a conserved surface overlapping the epitope of the Fab, and a distinctive variable motif. We suggest that the protein has a conserved function, possibly acting as a receptor or signal transducer.

MATERIALS AND METHODS

OspA–Fab 184.1 crystals were grown by vapor diffusion as described (20); they belong to space group $P2_12_12_1$, with unit cell dimensions $a = 89.2$ Å, $b = 91.7$ Å, and $c = 100.8$ Å. Diffraction data (Table 1) were collected at the Brookhaven National Laboratory National Synchrotron Light Source, on beamlines X25 (Cys-84-II) and X12C (all others). Each data set was collected from a single crystal soaked for 1–2 days in a cryoprotectant solution [50 mM Tris-HCl, pH 8.5/80 mM $MgCl_2/20\%$ PEG (M_r 3300)/8% glycerol] and then flash-cooled to 100 K. Platinum and lead derivatives were obtained by presoaking crystals in stabilizing solutions (no glycerol) containing millimolar concentrations of the heavy atom compounds; the iodine derivative was obtained by reacting the OspA–Fab 184.1 complex with Iodo-beads (Pierce) prior to crystallization. Diffraction images were collected using MAR image plate/scanner systems and were processed with DENZO (22).

When the HyHEL5 Fab (23) was used as a search model, a molecular replacement solution was independently obtained with both AMORE (24) and XPLOR (25–27). Phases calculated with the single platinum site identified by isomorphous and

The publication costs of this article were defrayed in part by page charge payment. This article must therefore be hereby marked “advertisement” in accordance with 18 U.S.C. §1734 solely to indicate this fact.

Copyright © 1997 by THE NATIONAL ACADEMY OF SCIENCES OF THE USA
0027-8424/97/943584-6\$2.00/0
PNAS is available online at <http://www.pnas.org>.

Abbreviation: OspA, outer surface protein A.
Data deposition: The atomic coordinates and structure factors have been deposited in the Protein Data Bank, Biology Department, Brookhaven National Laboratory, Upton, NY 11973 (reference 1OSP).

†Present address: California Institute of Technology, Division of Biology, mailcode 147–75, Pasadena, CA 91125.

§To whom reprint requests should be addressed.

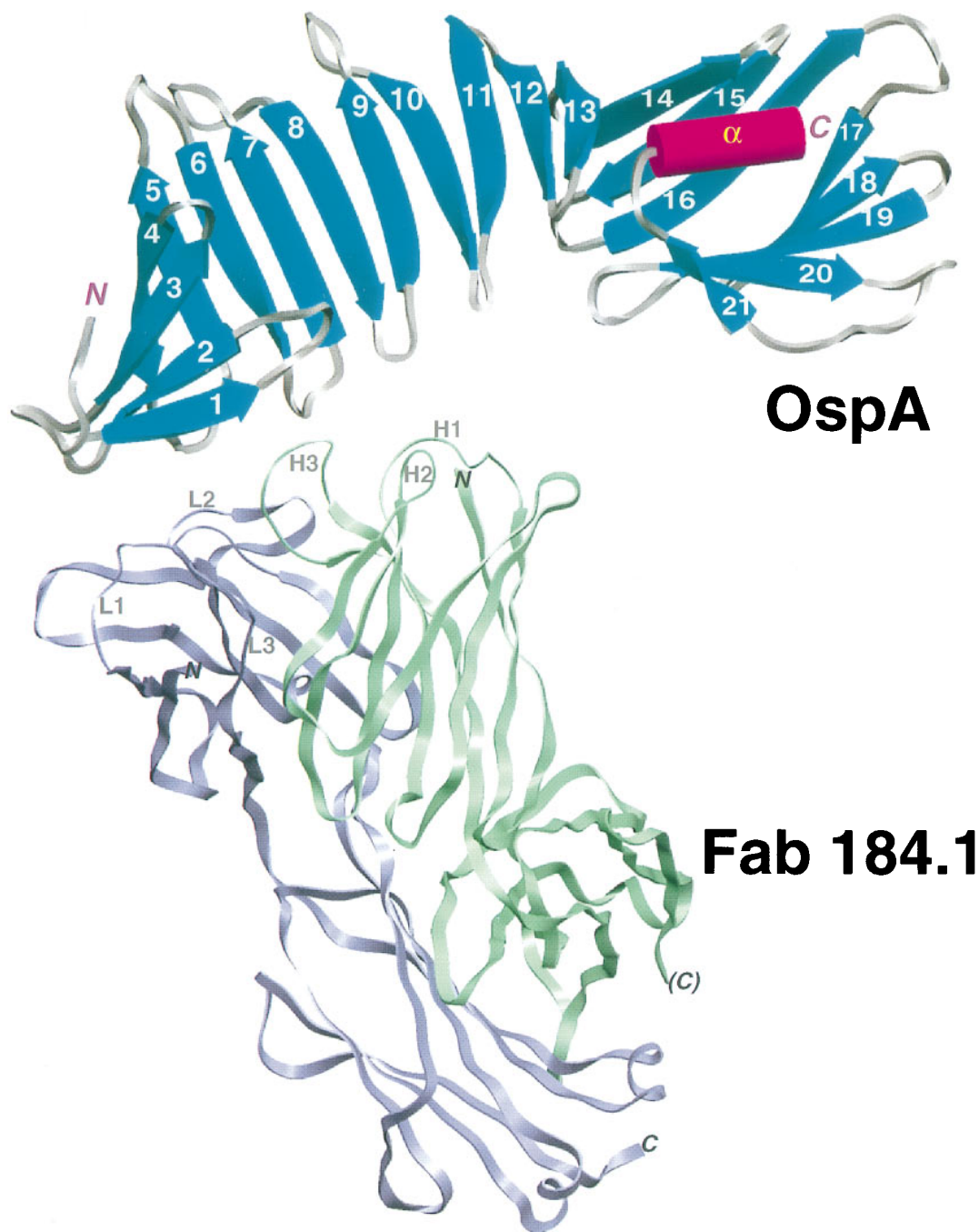


FIG. 1. Schematic view of the OspA–Fab 184.1 complex. OspA is displayed with its secondary structural elements, β -strands (cyan, numbered 1–21) and α -helix (magenta, labeled α), connected by grey turns or loops. The front face of the central sheet, as defined in the text, is seen in this view. Fab 184.1 is represented by violet and green ribbons for the light and heavy chains, respectively. The three complementarity determining region (CDR) loops on each chain are displayed as thin ropes and labeled (e.g., L1 for CDR1 of the light chain). The figure was generated with SETOR (21).

anomalous difference Patterson functions were employed to locate lead and iodine derivative sites; molecular replacement phased difference Fouriers provided independent verification of derivative sites. Several cycles of phase combination with SIGMAA (28), solvent flattening with SOLOMON (29), model building with O (30), followed by refinement with XPLOR were then performed. The assignment of side chains for the OspA polypeptide [strain B31 sequence (31)] was confirmed by difference Fourier maps locating the positions of two OspA site-directed point mutants (Ser-84 \rightarrow Cys and Ser-116 \rightarrow Cys: wild-type sequence and Cys-116 mutant data sets were collected but are not reported in Table 1). Diffraction data sets from OspA Cys-84 mutant crystals were of higher quality than

those of native OspA and so were ultimately used as parents in phasing calculations. The platinum compound bound to the sole methionine residue of OspA (Met-38); six iodine positions were located on tyrosine phenol rings of the Fab.

Recombinant OspA lacks the hydrophobic leader and signal peptidase II site of the native protein precursor (19). Ala-17, the mature recombinant N-terminal residue, replaces the mature native lipidated N-terminal Cys-17; the remainder of the recombinant polypeptide follows the OspA sequence (31). Electron density is not observed for the first six residues, so the OspA model extends from Ser-23 to Lys-273, the C terminus. The Fab model was generated by replacing the molecular replacement model with an immunoglobulin of class G2b and

Table 1. Diffraction data and phasing statistics for the OspA–Fab 184.1 complex

Dataset	Cys-84-I	Cys-84-II	K ₂ PtCl ₄	KI	Pb(CH ₃) ₃
Observed reflections, no.	155,965	254,719	87,304	70,488	89,601
Unique reflections, no.	36,731	58,870	20,837	17,419	23,461
Resolution limit, Å	2.30	1.95	2.80	2.85	2.70
Completeness, %*	97.9 (86.4)	97.1 (88.3)	98.2 (96.9)	88.5 (91.0)	99.3 (99.0)
R_{merge} , % [†]	5.2 (22.4)	4.8 (21.6)	8.0 (21.7)	8.6 (19.5)	6.9 (23.2)
R_{iso} , % [†]			6.8	10.5	6.6
Phasing power [‡]			1.61 (1.69)	1.24	1.09 (1.37)

*Data for reflections in the last shell for the given resolution limit are in parentheses. The shell width is ≈ 0.1 Å.

[†] R_{merge} indicates agreement of individual reflection measurements over the set of unique averaged reflections: $R_{\text{merge}} = \sum_h \sum_i |I(h)_i - I(h)| / \sum_h \sum_i I(h)_i$, where h is the Miller index and i indicates individual observed reflections, including those in symmetry equivalent positions. R_{iso} indicates agreement of native and derivative structure factors: $R_{\text{iso}} = \sum_h |F_P(h) - F_{PH}(h)| / \sum_h F_P(h)$.

[‡]Phasing power is the mean heavy-atom structure factor amplitude divided by the mean lack-of-closure error. Larger values usually indicate better calculated experimental phases. For platinum and lead derivatives, the phasing power for the anomalous component is given in parentheses.

then making substitutions according to Fab 184.1 light and heavy chain gene sequences that were determined by N-terminal sequencing followed by a reverse transcriptase-coupled polymerase chain reaction/sequencing method (No-

vagen). The final R factor for the OspA–Fab complex model refined against dataset Cys-84-II is 22.9% (R -free = 29.5%), with 5498 nonhydrogen atoms, including 328 water oxygens.

RESULTS AND DISCUSSION

Previous biophysical studies by France *et al.* (32) predicted predominantly β -structure for OspA. In the crystalline OspA–Fab 184.1 complex, OspA is folded into 21 consecutive antiparallel β -strands connected by turns or short loops, followed by a single C-terminal α -helix (Figs. 1 and 2). Ten β -strands (5–14n) form the molecule's scaffold: a long central β -sheet with right-handed twist. One edge of the central sheet is well-ordered with tight turns; the other edge is more poorly ordered with longer loops and β -bulges near the ends of three strands (Figs. 2 and 3). The repetitive fold of the central sheet is reminiscent of repetitive nonglobular structures—e.g., coiled-coils and leucine zippers. We designate the two faces of

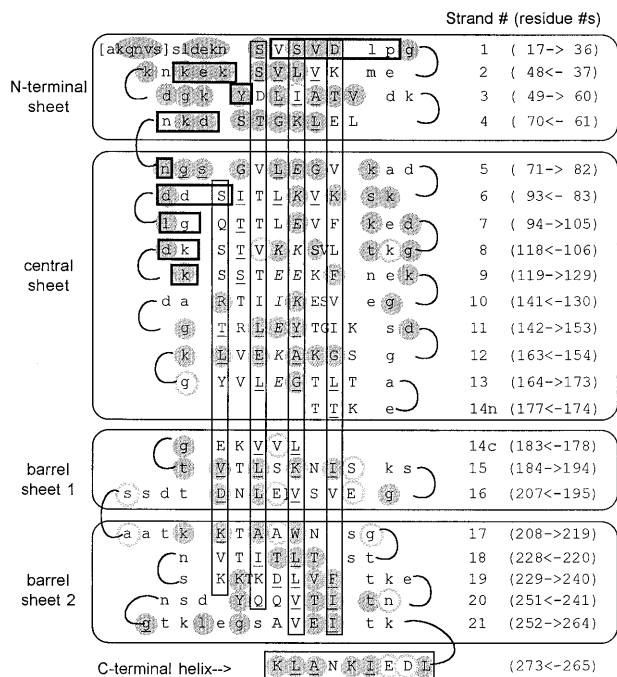


FIG. 2. Two-dimensional representation of the OspA folding pattern. The view is of the front face of the central β -sheet, with other β -sheets “uncurled” to form a single pseudocontinuous sheet. Residues in secondary structural elements (β -strands or α -helix) are represented by uppercase type; residues in turns are in lowercase type. Residues in brackets at the N terminus are predicted to be present in recombinant OspA but are not seen in the crystal. The four β -sheets formed by the 21 antiparallel β -strands are indicated by labeled rectangles enclosing sections of sequence, and the C-terminal α -helix is indicated at the bottom. For each line, the β -strand number is indicated in parentheses to the right, followed by the numerical range and direction of displayed residues. Vertical rectangles indicate residues with side chains extending behind the plane of the figure, residues with uppercase type outside the rectangles extend toward the viewer. Residues with exposed surface areas less than 10 \AA^2 are considered buried and are underlined. In general, buried residues are front-facing between strands 1 and 9 and rear-facing between strands 11 to 21, corresponding to the folding of N- and C-terminal domains on opposite sides of the central sheet. Strand 14 has main-chain hydrogen bonds to both the central sheet (14n) and to barrel sheet 1 (14c). Residues that contact Fab 184.1 are horizontally boxed (heavy lines); residues in the charge arrays are indicated in italic type. Residues strictly conserved in 49 OspA sequences (see Fig. 4) are within shaded circles; highly variable residues are within circles with shaded outlines.

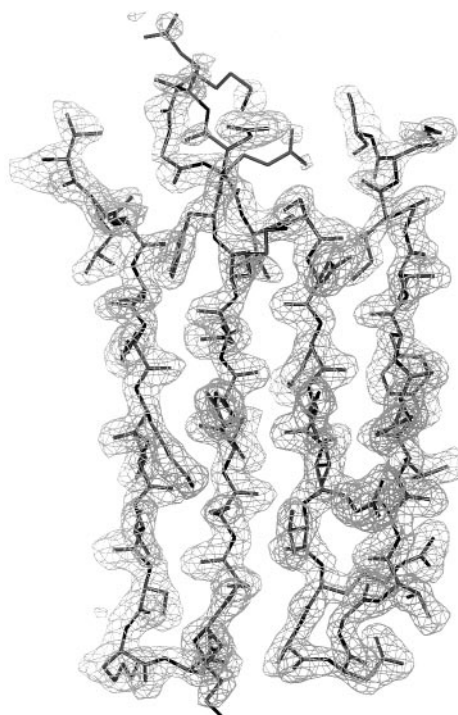


FIG. 3. Electron density for antiparallel β -strands 8–11 in the central sheet of OspA. The $(2F_{\text{obs}} - F_{\text{calc}})$ model phase map is contoured at 1.0σ (mesh). The thick-wire model extends from Thr-108 at the upper left through two β -hairpins to Ser-152 at the upper right. Note poor density for the flexible loop (upper center) between β -strands 9 and 10, typical for the larger more-flexible loops on the upper edge of the central sheet.

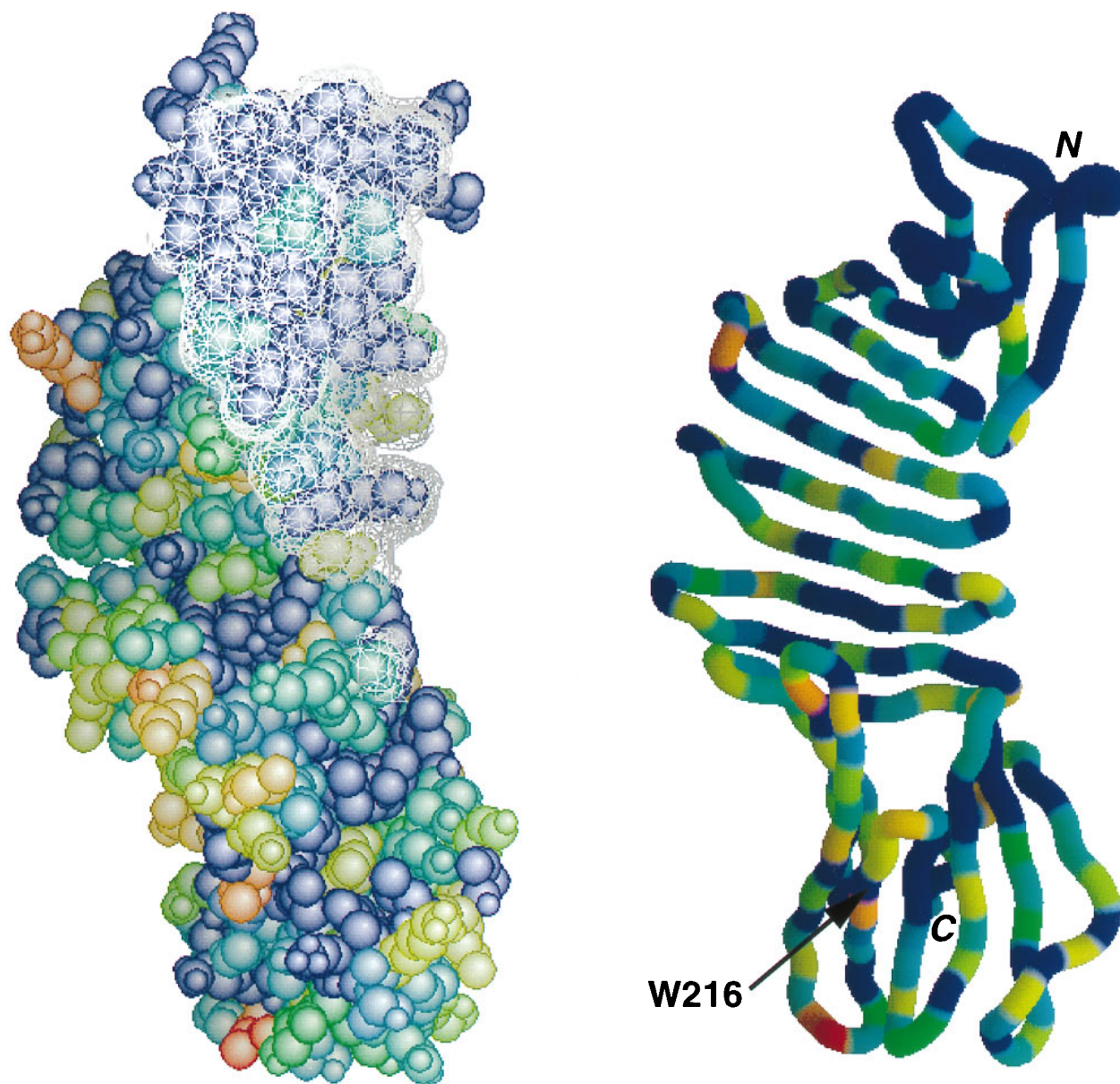


FIG. 4. Conservation map for OspA, with epitope of Fab 184.1 superimposed. Forty-nine OspA sequences available in GenBank in February 1996 were aligned, and the results were encoded on a 0–10 conservation scale using ALSRIPT (38). OspA was then color-coded according to conservation, with red representing the most variable residues and blue representing strictly conserved residues. Similar results are obtained when the 19 available OspB sequences are also included (data not shown). (Left) Space-filling model of OspA, with the surface made inaccessible by Fab 184.1 indicated as a white mesh. (Right) Ribbon model in same orientation, with same coloring scheme. Included were sequences from the genospecies *B. burgdorferi sensu stricto*, *Borrelia garinii*, *Borrelia afzelii*, *Borrelia japonica*, and *Borrelia andersonii* (16, 17). The figure was made with GRASP (39).

the central sheet as “front” and “back.” A small N-terminal β -sheet (strands 1–4) packs perpendicular to the first four strands of the front face, forming a β -sandwich domain. At the C-terminal end, two β -sheets (strands 14c–16 and 17–21) straddle the final α -helix to form a barrel-like unit that packs against the last five strands of the back face. Although the central sheet is involved in typical globular domain-packing arrangements at either end, three β -strands in the center (strands 8–10) are largely exposed to solvent on both faces. The latter feature appears to be unique among known protein structures; the distribution of residues in this region warrants careful inspection. OspA may prove to be a useful model for study of the folding of freestanding antiparallel β -sheets.

A large electrostatic component to the folding of recombinant OspA had been predicted based on the unusual stability of the protein at low and high salt concentrations and over a

wide pH range (32). In our model, all but three of 74 charged residues have surface-exposed charged groups forming ion pairs or higher-order arrays (the three exceptions are discussed later). An extended charge array composed of six side chains of alternating Glu and Lys residues is found on the back face of the central sheet, and an interrupted charge array (Lys, Glu, Ile, Glu, Lys, Glu) sits in an adjacent position on the front face (see Fig. 2, residues in italics). This arrangement bears resemblance to polar zippers predicted by Perutz and colleagues (33, 34) for primary sequences containing more obvious and extended regions of alternating charges. Although charged residues are known to be poor at forming antiparallel β -sheets by themselves, ion pairs across antiparallel β -strands have favorable side-chain interaction energies (35). Residues known to favor β -sheet formation, hydrophobic and uncharged polar residues (36, 37), flank the charge arrays. Alignment of

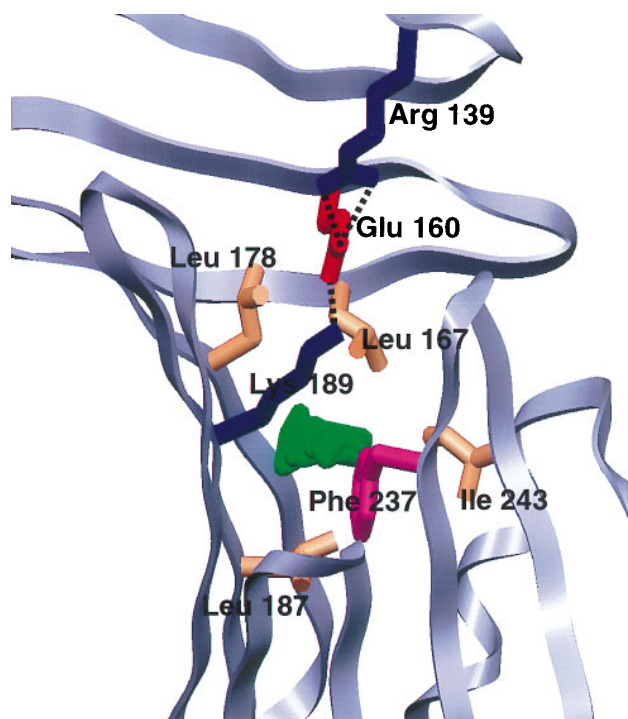


FIG. 5. Close-up of the C-terminal domain potential ligand binding pocket. The main chain of OspA is shown as a light-blue ribbon; residues forming the charge trio (Arg-139, Glu-160, and Lys-189) or lining the 34-Å³ cavity (Leu-167, Leu-178, Leu-187, Phe-237, and Ile-243) are shown in colors representative of side-chain type. The cavity, represented in green, was calculated by using the University of Groningen BIOMOL suite. The figure was generated with SETOR (21).

available OspA and OspB sequences (see Fig. 4) suggests that the charge arrays are not strictly conserved but continuous runs with four or more alternating charges always appear on at least one of the two faces. Charge arrays are likely to be an important feature in the stability of the central sheet antiparallel folding motif.

Monoclonal antibody 184.1 was raised against sonicated spirochetes (40). It recognizes an epitope near the N terminus of OspA that is not readily accessible on intact spirochetes (41). The Fab 184.1–OspA interface is typical of Fab–protein complexes (42), with extensive surface burial (800 Å² for OspA and 1200 Å² for the Fab), and intermolecular contacts that include seven direct hydrogen bonds, two ion pairs, numerous van der Waal's interactions, and water bridges. Consistent with the broad specificity of monoclonal antibody 184.1 (43), the epitope overlaps a highly conserved surface of OspA (Figs. 2 and 4). The size, shape, and *in vivo* inaccessibility of the conserved surface suggests that this region of OspA may normally take part in a specific interaction with another membrane component.

The C-terminal domain is the target of most agglutinating and neutralizing antibodies directed against OspA (44, 45); it must therefore be accessible on the spirochete cell surface. Mapping studies with OspA point mutants (46) have shown that the epitopes of three strain-specific agglutinating monoclonal antibodies as well as one broader-specificity neutralizing monoclonal antibody overlap a variable region in the C-terminal domain that includes a strictly conserved tryptophan residue (Trp-216). This region was predicted to adopt an α -helical conformation (47), but instead it encompasses two β -strands, 16 and 17, plus the loops flanking these strands (see Figs. 2 and 4). The discontinuity in main-chain hydrogen-bond formation between β -strands 16 and 17 provides significant surface exposure to most of the residues, a feature that might predispose the region to be antigenic. Conserved residues,

including Trp-216, face inward to form interstrand contacts. Residues that vary widely across the five defined genospecies of Lyme-disease-causing *Borrelia* (though are fairly well conserved within genospecies) are either outward-facing at the centers β -strands 16 and 17 or are exposed in the three loops flanking the two strands (Fig. 2). Significantly, the epitope of the protective monoclonal antibody LA-2 (48, 49) has recently been mapped to this hypervariable region (50). Success of recombinant OspA as a protective vaccine in a hamster model is strongly correlated with high titers of LA-2-equivalent antibodies (51). Thus, vaccines based on OspA may require representatives of this hypervariable region from several genospecies for world-wide effectiveness. To better define the epitope of LA-2, we have obtained crystals of OspA complexed with the LA-2 Fab fragment and structure determination is underway.

A prominent feature of the center of the C-terminal barrel domain is a trio of partially buried charged residues—Arg-139 from β -strand 10, Glu-160 from β -strand 12, and Lys-189 from β -strand 15 (Fig. 5). Of the three residues, the first two are strictly conserved in both OspA and OspB; position 189 is nearly always Lys in OspA and Arg in OspB. The trio is situated at the base of a well-conserved prominent cleft \approx 5 Å across, 24 Å long, and 8 Å deep. The cleft is formed in the C-terminal domain and is extended by curling of poorly ordered loops of the central sheet toward the back face, an effect promoted by β -bulges near the ends of β -strands 8, 10, and 11. The aliphatic side-chain methylenes of Lys-189 form the “lid” of a 34-Å³ solvent-inaccessible cavity that is lined by well-conserved hydrophobic residues (Fig. 5). Even though the cavity is large enough in volume to accommodate two solvent molecules, electron density maps do not indicate preferred water positions. The presence of the cavity and partially buried charges within the cleft suggests that the C-terminal domain of OspA might be a binding site for a ligand that could have a negative charge and certainly some hydrophobic character. We can only guess at the nature of the ligand, but the cleft is large enough to fit a small peptide, linear saccharide, or an exposed protein loop. Three-dimensional search programs (52–54) using either the whole OspA structure or the Arg-139, Glu-160, and Lys-189 motif as probes failed to find a similar arrangement of partially buried charged residues in other known protein structures.

We have described herein the structure of a protein of immunological interest for which there is no defined function. The usual question asked at the end of a structure determination, which is how does structure explain function, must be turned around—what does structure tell us about possible function? Although OspA has no significant sequence or structural homology to proteins with known function, we can still draw in a general way on known structure–function relationships. An extensive conserved surface usually denotes interactions with other macromolecules, and the presence of conserved charged groups in a pronounced cleft is typical of proteins that bind small or linear polymeric ligands. In its natural position in the spirochete, OspA could thus play a sensory role, e.g., recognizing either a soluble or host cell surface biomolecule in its C-terminal cleft and transmitting this information to another membrane component.

We are grateful to A. G. Murzin for recognizing the repetitive β -hairpin motif and pointing out the work of M. Perutz on polar zippers; P. Artymiuk and G. Vriend for performing three-dimensional homology searches; P. Freimuth for help with sequencing the Fab 184.1 genes; R. M. Sweet, M. S. Capel, and L. Berman for assistance at the National Synchrotron Light Source beamlines X12-C and X25; the National Cell Culture Center (Minneapolis) for antibody production; and F. T. Burling and V. L. Rath for discussions and helpful suggestions. The National Synchrotron Light Source is supported by the U.S. Department of Energy Office of Basic Energy Sciences. This research was conducted at Brookhaven National Laboratory with the

support of the National Institutes of Health (Grant RO1-AI37256), Brookhaven National Laboratory (Laboratory Directed Research and Development Grant 94-32), and the U.S. Department of Energy Office of Health and Environmental Research.

1. Barbour, A. G. & Fish, D. (1993) *Science* **260**, 1610–1616.
2. Barbour, A. G., Tessier, S. L. & Todd, W. J. (1983) *Infect. Immun.* **41**, 795–804.
3. Howe, T. R., Mayer, L. W. & Barbour, A. G. (1985) *Science* **227**, 645–646.
4. Howe, T. R., LaQuier, F. R. & Barbour, A. G. (1986) *Infect. Immun.* **54**, 207–212.
5. Brusca, J. S., McDowall, A. W., Norgard, M. V. & Radolf, J. D. (1991) *J. Bacteriol.* **173**, 8004–8008.
6. Skare, J. T., Shang, E. S., Foley, D. M., Blanco, D. R., Champion, C. I., Mirzabekov, T., Sokolov, Y., Kagan, B. L., Miller, J. N. & Lovett, M. A. (1995) *J. Clin. Invest.* **96**, 2380–2392.
7. Radolf, J. D., Goldberg, M. S., Bourell, K., Baker, S. I., Jones, J. D. & Norgard, M. V. (1995) *Infect. Immun.* **63**, 2154–2163.
8. Carroll, J. A. & Gherardini, F. C. (1996) *Infect. Immun.* **64**, 392–398.
9. Schwan, T. G., Piesman, J., Golde, W. T., Dolan, M. C. & Rosa, P. A. (1995) *Proc. Natl. Acad. Sci. USA* **92**, 2909–2913.
10. Fikrig, E., Barthold, S. W., Kantor, F. S. & Flavell, R. A. (1990) *Science* **250**, 553–556.
11. Fikrig, E., Barthold, S. W., Persing, D. H., Sun, X., Kantor, F. S. & Flavell, R. A. (1992) *J. Immunol.* **148**, 2256–2260.
12. Langermann, S., Palaszynski, S., Sadziene, A., Stover, C. K. & Koenig, S. (1994) *Nature (London)* **372**, 552–556.
13. de Silva, A. M., Telford, S. R., III, Brunet, L. R., Barthold, S. W. & Fikrig, E. (1996) *J. Exp. Med.* **183**, 271–275.
14. Stover, C. K., Bansal, G. P., Hanson, M. S., Burlein, J. E., Palaszynski, S. R., Young, J. F., Koenig, S., Young, D. B., Sadziene, A. & Barbour, A. G. (1993) *J. Exp. Med.* **178**, 197–209.
15. Keller, D., Koster, F. T., Marks, D. H., Hosbach, P., Erdile, L. F. & Mays, J. P. (1994) *J. Am. Med. Assoc.* **271**, 1764–1768.
16. Baranton, G., Postic, D., Saint Girons, I., Boerlin, P., Piffaretti, J. C., Assous, M. & Grimont, P. A. (1992) *Int. J. Syst. Bacteriol.* **42**, 378–383.
17. Postic, D., Assous, M. V., Grimont, P. A. & Baranton, G. (1994) *Int. J. Syst. Bacteriol.* **44**, 743–752.
18. Brandt, M. E., Riley, B. S., Radolf, J. D. & Norgard, M. V. (1990) *Infect. Immun.* **58**, 983–991.
19. Dunn, J. J., Lade, B. N. & Barbour, A. G. (1990) *Protein Expression Purif.* **1**, 159–168.
20. Li, H. & Lawson, C. L. (1995) *J. Struct. Biol.* **115**, 335–337.
21. Evans, S. V. (1993) *J. Mol. Graphics* **11**, 134–138.
22. Otwinowski, Z. (1993) in *Proceedings of the CCP4 Study Weekend: Data Collection and Processing*, eds. Sawyer, L., Isaacs, N. & Bailey, S. (Science and Engineering Research Council, Daresbury Laboratory, Warrington, U.K.), pp. 56–62.
23. Sheriff, S., Silverton, E. W., Padlan, E. A., Cohen, G. H., Smith-Gill, S. J., Finzel, B. C. & Davies, D. R. (1987) *Proc. Natl. Acad. Sci. USA* **84**, 8075–9079.
24. Navaza, J. (1994) *Acta Crystallogr. A* **50**, 157–163.
25. Brünger, A. T., Kuriyan, J. & Karplus, M. (1987) *Science* **235**, 458–460.
26. Brünger, A. T. (1990) *Acta Crystallogr. A* **46**, 46–57.
27. Brünger, A. T. (1992) *Nature (London)* **335**, 472–475.
28. Read, R. J. (1986) *Acta Crystallogr. A* **42**, 140–149.
29. Abrahams, J. P., Leslie, A. G. W., Lutter, R. & Walker, J. E. (1994) *Nature (London)* **370**, 621–628.
30. Jones, T. A., Zou, J. Y., Cowan, S. W. & Kjeldgaard, M. (1991) *Acta Crystallogr. A* **47**, 110–119.
31. Bergström, S., Blundoc, V. G. & Barbour, A. G. (1989) *Mol. Microbiol.* **3**, 479–486.
32. France, L. L., Kieleczawa, J., Dunn, J. J., Hind, G. & Sutherland, J. C. (1992) *Biochim. Biophys. Acta* **1120**, 59–68.
33. Perutz, M. F., Staden, R., Moens, L. & De Baere, I. (1993) *Curr. Biol.* **3**, 249–253.
34. Perutz, M. F. (1994) *Protein Sci.* **3**, 1629–1637.
35. Smith, C. K. & Regan, L. (1995) *Science* **270**, 980–982.
36. Kim, C. A. & Berg, J. M. (1993) *Nature (London)* **362**, 267–270.
37. Minor, D. L., Jr., & Kim, P. S. (1994) *Nature (London)* **367**, 660–663.
38. Barton, G. J. (1993) *Protein Eng.* **6**, 37–40.
39. Honig, B. & Nicholls, A. (1995) *Science* **268**, 1144–1149.
40. Jiang, W., Luft, B. J., Munoz, P., Dattwyler, R. J. & Gorevic, P. D. (1990) *J. Immunol.* **144**, 284–289.
41. Schubach, W. H., Mudri, S., Dattwyler, R. J. & Luft, B. J. (1991) *Infect. Immun.* **59**, 1911–1915.
42. Davies, D. R. & Cohen, G. H. (1996) *Proc. Natl. Acad. Sci. USA* **93**, 7–12.
43. Jiang, W., Gorevic, P. D., Dattwyler, R. J., Dunn, J. J. & Luft, B. J. (1994) *Clin. Diagn. Lab. Immunol.* **1**, 406–412.
44. Wilske, B., Luft, B. J., Schubach, W. H., Zumstein, G., Jauris, S., Preac-Mursic, V. & Kramer, M. D. (1992) *Med. Microbiol. Immunol.* **181**, 191–207.
45. Sears, J. E., Fikrig, E., Nakagawa, T. Y., Deponte, K., Marcantonio, N., Kantor, F. S. & Flavell, R. A. (1991) *J. Immunol.* **147**, 1995–2000.
46. McGrath, B. C., Dunn, J. J., Gorgone, G., Guttman, D., Dykhuizen, D. & Luft, B. J. (1995) *Infect. Immun.* **63**, 1356–1361.
47. France, L. L., Kieleczawa, J., Dunn, J. J., Luft, B. J., Hind, G. & Sutherland, J. C. (1993) *Biochim. Biophys. Acta* **1202**, 287–296.
48. Schaible, U. E., Kramer, M. D., Eichmann, K., Modolell, M., Museteanu, C. & Simon, M. M. (1990) *Proc. Natl. Acad. Sci. USA* **87**, 3768–3772.
49. Simon, M. M., Schaible, U. E., Kramer, M. D., Eckerskorn, C., Museteanu, C., Muller-Hermelink, H. K. & Wallich, R. (1991) *J. Infect. Dis.* **164**, 123–132.
50. Rubenbauer, F. V. (1996) Masters thesis (C. W. Post College, Long Island University, Brookville, NY).
51. Johnson, B. J. B., Sviat, S. L., Happ, C. M., Dunn, J. J., Frantz, J. C., Mayer, L. W. & Piesman, J. (1995) *Vaccine* **13**, 1086–1094.
52. Holm, L. & Sander, C. (1995) *Trends Biochem. Sci.* **20**, 478–480.
53. Artymiuk, P. J., Poirrette, A. R., Grindley, H. M., Rice, D. W. & Willett, P. (1994) *J. Mol. Biol.* **243**, 327–344.
54. Vriend, G. (1990) *J. Mol. Graphics* **8**, 52–56.